Molecular Crystals and Liquid Crystals
Publication details, including instructions for authors and subscription information:
http://www.tandfonline.com/loi/gmcl20

Spontaneous Formation of Polar Liquid Crystal in Lyotropic Solution of Helical Poly(γ-Benzyl Glutamate)

Chu-Chu Yen [a] , Yoshiaki Taguchi [a] , Masatoshi Tokita [a] & Junji Watanabe [a]

[a] Department of Organic and Polymeric Materials, Tokyo Institute of Technology, Ookayama, Meguro-ku, Tokyo, Japan

Version of record first published: 22 Feb 2010

To cite this article: Chu-Chu Yen, Yoshiaki Taguchi, Masatoshi Tokita & Junji Watanabe (2010): Spontaneous Formation of Polar Liquid Crystal in Lyotropic Solution of Helical Poly(γ-Benzyl Glutamate), Molecular Crystals and Liquid Crystals, 516:1, 91-98

To link to this article: http://dx.doi.org/10.1080/15421400903400712

Mol. Cryst. Liq. Cryst., Vol. 516: pp. 91–98, 2010

ISSN: 1542-1406 print/1563-5287 online
DOI: 10.1080/15421400903400712

Spontaneous Formation of Polar Liquid Crystal in Lyotropic Solution of Helical Poly(γ-Benzyl Glutamate)

CHU-CHU YEN, YOSHIAKI TAGUCHI,
MASATOSHI TOKITA, AND JUNJI WATANABE

Department of Organic and Polymeric Materials, Tokyo Institute
of Technology, Ookayama, Meguro-ku, Tokyo, Japan

In this study, we are concerned with the important characteristic in biological polypeptide helices, polarity. Through the observation of second harmonic generation (SHG) effect, we first show that a polar packing structure is spontaneously formed in solid films of the typical helical polypeptide, poly(γ-benzyl L-glutamate) (PBLG) which were cast from the form B solvents. Secondly, we present the spontaneous formation of polar nematic phase in lyotropic liquid crystal (LC) solutions of PBLG and poly(γ-benzyl D-glutamate) (PBDG) mixture and the polar-to-nonpolar transition upon increasing the temperature or decreasing the concentration of the solutions. The huge dipole moment of PBG molecule resulting from the accumulation of residue dipole component is attributable to the unusual formation of the polar nematic phase. The decisive evidence of polar liquid crystal open a new field on LCs, and possess the potentiality of the self-organization into the polar packing which may serve as electric devices in living systems.

Keywords Polarity; polar liquid crystal; polar nematic; polar-to-nonpolar transition; poly(benzyl glutamate); polypeptide; second-harmonic generation

Introduction

Rigidity and chirality are the topical characteristics of α-helical polypeptides [1]. These two characteristics are the cause of the natural tendency for polypeptide molecules to form a chiral nematic (or cholesteric) LC in concentrated solutions [2,3]. The transition behavior from isotropic to LC solution and the structural feature of the resulting superhelicoidal cholesterics have been significant research subjects for clarifying the self organization of biological polymers in a living system [4,5].

In addition to rigidity and chirality, one of another significant feature is that the helical polypeptide is the macro-dipolar molecule. Since the helical conformation of polypeptides is built up by regular intramolecular hydrogen bonds between the N−H and C=O groups, there is a direct addition of residue dipole components along the polymer chain, producing a huge dipole moment, μ (for example, $\mu =$ ca. 500D for an

---

Address correspondence to Masatoshi Tokita, Department of Organic and Polymeric Materials, Tokyo Institute of Technology, Ookayama, Meguro-ku, Tokyo 152-8552, Japan. E-mail: mtokita@polymer.titech.ac.jp

α-helical PBLG with a molecular weight, M_w of 30,000) [6]. This huge dipole moment is attractive because of the potentiality of forming polar or ferroelectric LCs although only a few researchers have been concerned with studies on subjects related to the polar packing of the polar polypeptides [7–9].

Recently, however, theoretical investigations [10–12] and computer simulation [13] have suggested that rigid-rod polymers, if they have a huge dipole moment along their long axis like PBLG, can form a polar packing structure in their LCs. In this study, we give the experimerntal evidence of polar nematic LC from the SHG measurement, which will open a new research field on LCs and provide new insights into the biological importance of polar structure in supermolecularly associated materials of living systems composed of fibrous proteins, polysaccharides and DNA.

Experimental

PBLG and PBDG polymers were prepared by standard N-carboxyl anhydride (NCA) method. Wide-angle X-ray diffraction measurements were performed by using a Rigaku-Denki RU-200BH X-ray generator with Ni-filtered CuKα radiation. SHG was used as a probe to monitor the spontaneous polarization in the medium [9]. Q-switched Nd: YAG laser light (1064 nm) was incident perpendicular to the films (illumination area; 0.1 mm in diameter) after passing through a quarter-wave plate and a polarizer. SH light (532 nm) generated from the sample was detected by a Hamamatsu model-R955 photomultiplier tube in a transmitted direction after passing through an IR cut filter, an interference filter and an analyzer. The SH light intensity was measured as a function of the rotation angle of the polarizer or analyzer.

Results and Discussion

1. *SHG-Active Polar Structure Observed in Solid Films Cast from Lyrotropic LC Solutions*

With respect to the polarity, we recall the interesting fact that there are two crystal modifications, *forms B* and *C*, in PBLG films [14]. These forms are prepared by casting from different kinds of solvents. From the polar solvents such as N,N-dimethylformamide (DMF) and benzyl alcohol, the *form B* is obtained, while *form C* is formed from solvents like chloroform and ethylene dichloride (EDC). *Form B* has a well-defined crystalline structure with a three-dimensional monoclinic unit cell [14,15], while *form C* shows a poor packing periodicity [15]. Of interest is the fact that the packing feature of these two forms is not altered at all by annealing at high temperatures above 150°C, where the side chains are freely rotated. This means that the difference in the packing structure cannot be attributed to a difference in side-chain conformation that may be induced by some specific interaction between side chains and solvents. Thus, we consider another structural factor, the "Up" and "Down" arrangement of polar molecules; it may be regular in *form B*, but irregular in *form C* [15]. SHG measurement will likely be the simplest method to clarify whether the polar (or non-centrosymmetric) packing exists or not [16].

We first prepared the oriented films of PBLG ($M_w = 27{,}000$) for the analysis of SHG. Two types of film with high orientation were obtained by applying an external

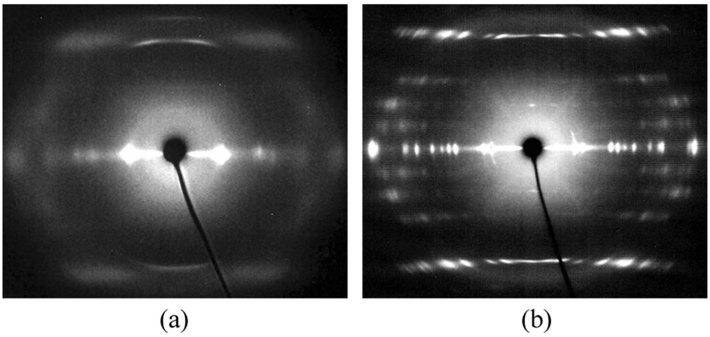

Figure 1. X-ray diffraction photographs of oriented PBLG ($M_w = 27{,}000$) films prepared from liquid crystal solutions in EDC (15 wt%). The highly oriented samples were obtained under (a) magnetic (5 Tesla) and (b) electric (0.6 V/μm) fields. The molecular long axis corresponding to the field direction is set along the vertical direction.

electric (0.6 V/μm) and magnetic field (5 Tesla) to lyotropic solutions (15 wt%) in EDC (*form C* solvent). The X-ray patterns are shown for the magnetically and electrically oriented films in Figures 1(a) and (b), respectively. The magnetically aligned film (Fig. 1(a)) shows the hexagonal pattern characteristic of *form C* with broad reflections on the equatorial line and diffuse streaks on the layer lines. The equatorial reflections with spacings of 12.8, 7.28, and 6.39 Å indicate the molecular packing with the pseudo-hexagonal lattice of a = b = 14.8 Å with its chains displaced randomly along their chain axes. The turn layer reflections near 5.3 Å and the 1.5-Å meridional reflection accounted for the α-helical conformation with 18 residues in 5 turns. An SHG signal is not detected at all from this oriented *form C* film, which ensures that the α-helices in the *form C* film are placed randomly with respect to their "Up" and "Down" directionality.

In contrast, the electrically aligned one shows the well-defined crystalline X-ray pattern in Figure 1(b) irrespective of the use of the same *form C* solvent. It includes many sharp reflections, which can be indexed into a three-dimensional monoclinic lattice containing two chains with lattice parameters of a = 29.0 Å, b = 13.4 Å, c = 26.9 Å, $\alpha = \gamma = 90°$, and $\beta = 96°$. This result is remarkable since the crystal structure agrees exactly with that of *form B*, which can be formed from DMF *form B* solvent [15]. Figure 2 shows the polar SHG intensity profiles obtained with the different angular combinations of the polarizer and analyzer. The relatively strong SHG signals indicate that the electrical poling by the electric field of 0.6 V/μm is successful in inducing the non-centrosymmetry of molecular packing [17], that is, polar packing with the same "Up" or "Down" directionality. As given by the solid curves in Figure 2, the intensity profiles are well fitted by the C_s symmetry attributable to the polar monoclinic lattice. We thus reach the important conclusion that the polar packing of molecules forced by electric poling results in *form B* crystal even if the *form C* solvent is used.

The magnetically oriented film was also prepared from the DMF *form B* solvent at 50°C. The orientation is not good in this case because of the strong twisting power of cholesteric LC in the DMF solvent [18]. Irrespective of this ambiguity, the SHG signal is clearly detected for this *form B* film with a similar intensity as that in the electrically poled film from *form C* solvent. The simple DMF-cast film also shows

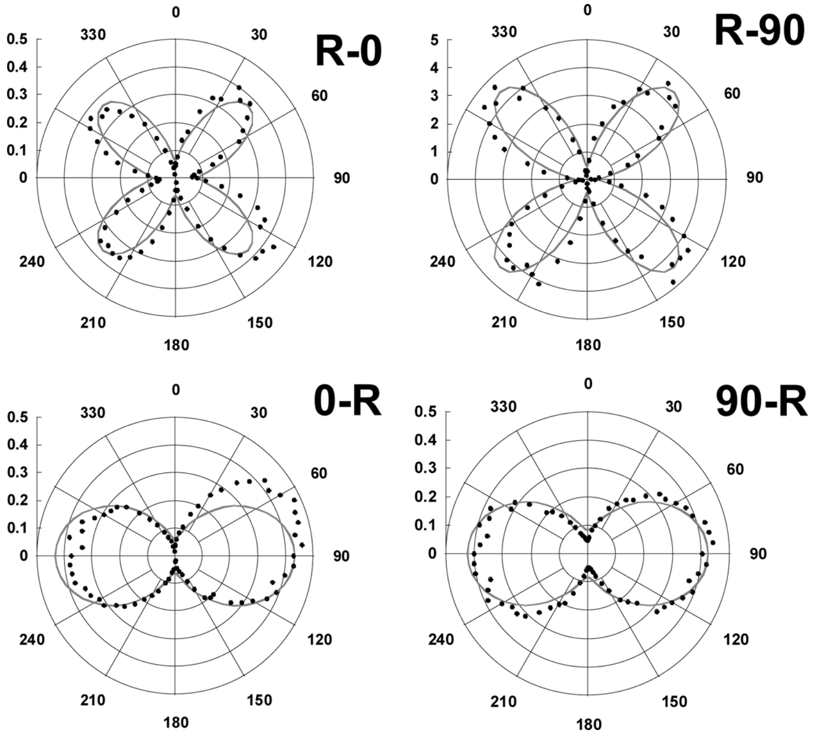

Figure 2. Intensity profiles of SHG light observed for the electrically aligned PBLG film from EDC solution, with various angular combinations of φ_p and φ_a. Intensities are polar-plotted with four configurations of R-0, R-90, 0-R, and 90-R. Combinations of R-0 and R-90 indicate that the polarization of fundamental light is rotated about the beam direction (i.e., $R = \varphi_p$ varied from 0° to 360°), while the analyzer angle for SHG φ_a is fixed at 0° and 90°, respectively. The combinations of 0-R and 90-R indicate that the analyzer direction ($R = \varphi_a$) is rotated with φ_p fixed at 0° and 90°, respectively. The clockwise rotation is defined as the view along the beam and the molecular polar axis is set to be 0°. The solid curves show the validity of our theoretical calculations based on C_s symmetry. The determined second-order nonlinear optical susceptibility (χ) parameters are as follows: $\chi_{11}+\chi_{12}=1.7$, $\chi_{13}=3.7$, $\chi_{26}=2.8$, $\chi_{15}+\chi_{24}=16.0$, $\chi_{31}+\chi_{32}=2.3$, $\chi_{33}=1.0$ and $\chi_{35}=3.1$.

the clear SHG signal [8]. These results lead to another interesting conclusion: in *form B* from DMF and benzyl alcohol solutions, polypeptide molecules can be self-organized into the polar packing structure without electric poling.

2. *Formation of Polar Nematic LC in Lyotropic Solution*

Above results strongly suggest that the polar structure may be formed in the preceding lyotropic LC solution of the *form B* solvent is used. To clarify this point, we will perform a direct SHG observation for the LC solutions with various concentrations.

We used here a racemic mixture of PBLG ($M_w = 420{,}000$) and PBDG ($M_w = 490{,}000$) which can form a nematic LC, to avoid the formation of the complex cholesteric helix in the enantiomeric PBLG system [8]. The racemic mixture is called here PBG. The benzyl alcohol (BA) solvent was used as a *form B* solvent since it has

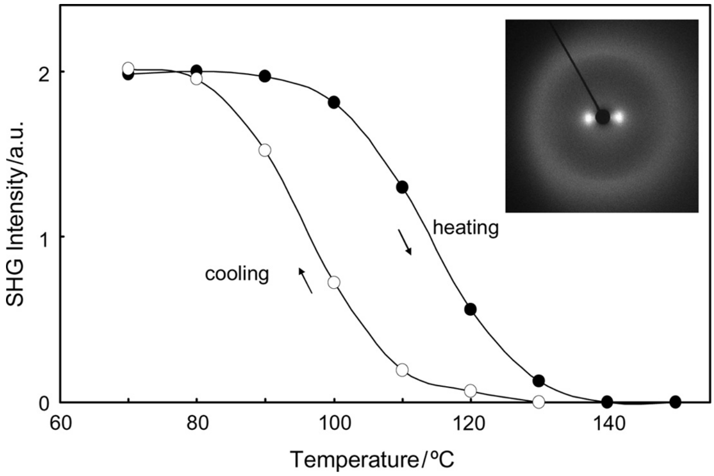

Figure 3. SHG response from nematic PBG solution in BA on heating and cooling cycle. The solution with concentration of 28.2 wt% was kept inside a capillary tube with a diameter of 1 mm and the SHG response was then observed for the monodomain nematic solution aligned uniaxially under the magnetic field. The inset shows the X-ray pattern taken for the magnetically aligned nematic solution at 140°C.

a high boiling point of 205°C which allows the observation of the SHG response in the solutions over a wide temperature range. The LC solutions were prepared with various concentrations from 15 wt% to 45 wt%.

The nematic solutions were kept inside a capillary tube with a diameter of 1 mm and placed under the magnetic filed. The perfect orientation of nematic LCs can be detected in the X-ray pattern as shown in the inset of Figure 3. The SHG measurement was then performed for this highly aligned monodomain solutions to eliminate the artificial SHG effect from the domain surface [19]. Figure 3 shows the temperature dependence of SHG intensity, which is typically observed for the solution with 28.2 wt% concentration. As envisaged above, the SHG response is clearly detected at low temperatures around 80°C. However, SHG intensity decreases upon heating and disappears at temperatures higher than 140°C. Upon cooling, the SHG intensity recovers to its initial value at 80°C. A hysteresis effect can be seen upon heating and cooling. This may be partly because the annealing time of 30 min for each data point is not sufficient for a thermodynamic equilibrium. The optical microscopic and X-ray observations show that the nematic LC is stable in the experimental temperature region. Thus, Figure 3 represents not only the formation of the polar nematic structure in the lyotropic LC solutions, but also the temperature-induced transformation from polar to nonpolar LC.

All the nematic solutions prepared with various concentrations from 20 to 45 wt% show the similar temperature dependence of SHG response as shown in Figure 4, clarifying a clear trend that the polar-to-nonpolar transition (instability) temperature is increased from 85 to 160°C with an increase in concentration. The instability temperatures, together with the well-known chimney type of coexisting region of isotropic and nematic phases [2,20], are given in the temperature-concentration phase diagram of Figure 5. At relatively high temperatures, the nonpolar nematic LC initially appears from the isotropic solution and the

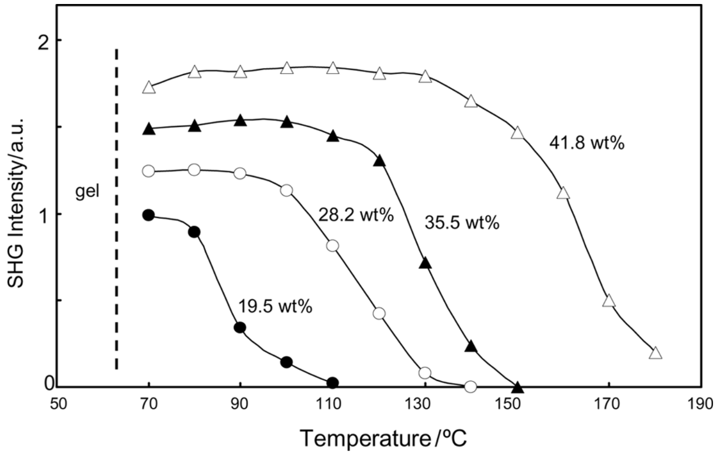

Figure 4. Temperature dependence of SHG intensity for nematic PBG solutions with various concentrations from 19.5 to 41.8 wt%. The data were collected during heating.

nonpolar-to-polar transition takes place with increasing concentration (shown by the arrow in Fig. 5). Since the present PBG molecules with a large axial ratio of 200 cannot easily rotate around their short axis to change the head-tail direction, the nonpolar-to-polar transformation proceeds by a simple migration of polypeptides in such a way that those with the same directionality gather together to form the polar domain (refer to the illustration in inset of Fig. 5). It may be a kind of phase

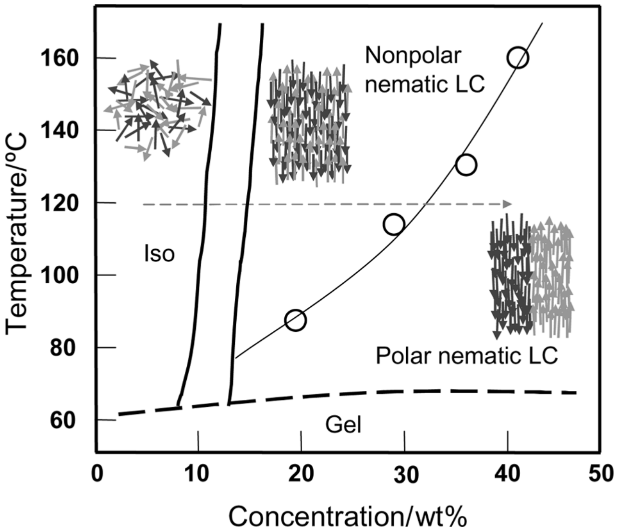

Figure 5. Phase diagram of lyotropic PBG solution in BA in the temperature-concentration plane, including the polar-to-nonpolar temperature, T_c, plotted by open circles, and the isotropic-nematic coexistence region of 10 to 13 wt% given by solid curves. At temperatures lower than 60°C, solutions form the whitish gel. When the concentration of solution increases along the arrow, the nonpolar nematic phase initially appears from the isotropic phase and then transforms to the polar nematic one. Its schematic illustration is given in the inset.

separation; the time required for the nonpolar-to-polar transformation in the solution of 28.2 wt% concentration was estimated as ~12 min from the time dependence of the SHG intensity recovering upon the temperature jump from 150 to 80°C. Figure 5 also shows that in the limited temperature region of 60 to 75°C, the system goes directly from the isotropic to the polar nematic phase. The three phases then coexist at a triple point of ~13 wt% and 75°C [11–13].

In conventional nematic LCs, polar-to-nonpolar temperature, T_c, can be predicted by the equation [10]

$$T_e \sim (d/l)\rho m^2/k_\mathrm{B}.$$

Here, d is the diameter of the molecule, l the length of the molecule, ρ the number density, and m the longitudinal dipole moment of the rodlike molecule. For typical low-molecular-weight molecules, $m \sim 1$ D and $\rho \sim 2 \times 10^{21}\,\mathrm{cm}^{-3}$, and then $T_c \sim 1$ K. This indicates that at realistic temperatures thermal molecular motion destroys the ferroelectric polar ordering. On the same basis, ferroelectric ordering would be possible if molecules have a dipole moment m as large as 10 D [10,12]. Such large values of m are possible only in polar polymers like α-helical polypeptides [21] and aromatic polyesters [9,22]. For the present PBG with the degree of polymerization of ~2000, for example, m is roughly 8000 D, d/l is 5×10^{-3}, ρ is approximately $3 \times 10^{17}\,\mathrm{cm}^{-3}$ for the solution of 30 wt% concentration, and then $T_c \sim 10^2$ K. This is a sufficiently high temperature that can explain the present results, i.e., the formation of the polar structure in a realistic temperature region and the polar-to-nonpolar transition with the temperature variation. The increase in T_c with concentration can be attributed to the increase in ρ.

Conclusion

As a conclusion, we present the spontaneous formation of polar nematic phase and the polar-to-nonpolar transition upon increasing the temperature or decreasing the concentration in lyotropic liquid crystal solutions of helical PBG. The interplay between the polymeric and liquid crystalline effects, that is a coupling of the rigidity and the huge dipole moment of PBG molecule, is attributable to the unusual formation of the polar nematic phase. Similar principles may apply to the self-ordering of biological macromolecules in living material systems, including polysaccharides such as cellulose and chitin, fibrous proteins such as keratin and collagen, and DNA, which reminds us of another topical feature, polar ordering of biological macromolecules in the LC field that may induce piezoelectricity and pyroelectricity of materials in living systems.

References

[1] Pauling, L. & Corey, R. B. (1950). *J. Am. Chem. Soc.*, *72*, 5349.

[2] Flory, P. J. (1956). *Proc. R. Soc.*, *A234*, 60–89.

[3] Robinson, C. (1956). *Trans. Faraday Soc.*, *52*, 571–592.

[4] Kelker, H. & Hatz, R. (1980). *Handbook of Liquid Crystals*, Veinheim, Verlag Chemie: Deerfield, 553–592.

[5] Bouligand, Y. (1978). In: *Liquid Crystalline Order Polymers*, Blumstein, A. (Ed.), Academic: New York, 262–298.

[6] Wada, A. (1976). *Adv. Biophys.*, *9*, 1–63.

[7] Park, B., Kinoshita, Y., Takezoe, H., & Watanabe, J. (1998). *Jpn. J. Appl. Phys.*, *37*, L136–138.

[8] Watanabe, J., Hirose, Y., Tokita, M., Watanabe, T., & Miyata, S. (1998). *Macromolecules*, *31*, 5937–5939.

[9] Watanabe, T., Miyata, S., Furukawa, T., Takezoe, H., Nishi, T., Sone, M., Migita, A., & Watanabe, J. (1996). *Jpn. J. Appl. Phys.*, *35*, 1505–1507.

[10] Terentjev, E. M., Osipov, M. A., & Sluckin, T. J. (1994). *J. Phys. A*, *27*, 7047–7059.

[11] Groh, B. & Dietrich, S. (1997). *Phys. Rev. E*, *55*, 2892–2901.

[12] Yu, C-J., Yu, M., & Lee, S-D. (2002). *Jpn. J. Appl. Phys.*, *41*, L102–104.

[13] Biscarini, F., Zannoni, C., Chiccoli, C., & Pasini, P. (1991). *Mol. Phys.*, *73*, 439–461.

[14] Samulski, E. T. & Tobolsky, A. (1967). *Nature*, *216*, 997; Mckinnon, A. J. & Tobolsky, A. V. (1968). *J. Phys. Chem.*, *72*, 1157–1161.

[15] Watanabe, J., Imai, Z., Gehani, R., & Uematsu, I. (1981). *J. Polym. Sci. Polym. Phys. Ed.*, *19*, 653–665.

[16] Prasad, P. N. & Williams, D. J. (1991). *Introduction to Nonlinear Optical Effects in Molecules & Polymers*, John Wiley & Sons: New York.

[17] Levine, B. F. & Bethea, C. G. (1976). *J. Chem. Phys.*, *65*, 1989–1993.

[18] Uematsu, I. & Uematsu, Y. (1984). *Adv. Polym. Sci.*, *59*, 37–73.

[19] Prasad, P. N. & Williams, D. J. (1991). *Introduction to Nonlinear Optical Effects in Molecules & Polymers*, John Wiley & Sons: New York.

[20] Yen, C.-C., Edo, S., Oka, H., Tokita, M., & Watanabe, J. (2008). *Macromolecules*, *41*, 3727–3733.

[21] Yen, C.-C., Tokita, M., Park, B., Takezoe, H., & Watanabe, J. (2006). *Macromolecules*, *39*, 1313–1315.

[22] Koike, M., Yen, C.-C., Yuqing, L., Tsuchiya, H., Tokita, M., Kawauchi, S., Takezoe, H., & Watanabe, J. (2007). *Macromolecules*, *40*, 2524–2531.